6th International Conference on CFD in Oil & Gas, Metallurgical and Process Industries
SINTEF/NTNU, Trondheim NORWAY *CFD08-102*
10-12 June 2008

ACCURACY OF BUBBLE VELOCITY MEASUREMENT WITH A FOUR-POINT OPTICAL FIBRE PROBE

Wei BAI[1], Niels G. DEEN[1]*, Robert F. MUDDE[2] AND J.A.M. KUIPERS[1]

[1] Fundamentals of Chemical Reaction Engineering, Faculty of Science and Engineering
Institute of Mechanics, Processes and Control Twente (IMPACT),
University of Twente, 7500 AE Enschede, The Netherlands

[2] Kramers Laboratorium voor Fysische Technologie, Delft Univ. of Technology, 2628 BW Delft, The Netherlands

* Corresponding author, e-mail: N.G.Deen@utwente.nl

ABSTRACT

For the operation of high void fraction bubbly flows in bubble columns, insight in primary parameters such as bubble size, shape and velocity as well as gas volume fraction is essential. At high gas volume fractions the flow system becomes opaque, ruling out non-intrusive optical techniques. As an alternative optical fibre probes can be used, which have the advantage of low cost, simplicity of setup and easy interpretation of the results.
By using four-point optical fibre probe, properties of bubbles can be studied, such as bubble velocity, bubble size, etc. However, the effect of bubble wobbling behaviour and physical properties of liquids on the accuracy of the velocity measurements has not been investigated in detail.
In the present study, the performance of a four-point optical fibre probe was evaluated for five different liquids. The probe performance and causes of inaccuracies are discussed.

Keywords: Bubble column, four-point optical fibre probe, CMOS camera.

NOMENCLATURE

p	Fraction of pixels [-]
Pr	The probability [-]
Δs	distance between the longest tip and the other three tips [m]
Δt	average time difference between bubble hitting the longest tip and the other three tips [s]
u	velocity from four-point optical fibre probe [m/s]
v	vertical velocity of bubble [m/s]
V_{entry}	voltage of probe entering bubble [V]
V_{exit}	voltage of probe exiting bubble [V]
y	vertical position of bubble [m]
w_0 , w_1	class occurrence [-]
m_0 , m_1	class mean [-]
m_T	total mean level [-]
s_B	between-class variance [-]
b	bubble selection criterion [-]

INTRODUCTION

For the operation of bubbly flows at high void fraction, insight in primary parameters such as bubble size, shape and velocity as well as volume fraction is essential.
Direct optical techniques i.e. particle image velocimetry (Lindken and Merzkirch, 1999, Deen, 2001, Bröder and Sommerfeld, 2002) or laser Doppler anemometry, which are commonly used in gas-liquid flows, are only applicable in bubbly flows at relatively low gas hold-up. With void fraction increasing, these methods face problems of reflection and refraction.
Some other techniques, such as, X-ray and gamma-ray tomography can be used as an alternative. However, the cost of these techniques is considerable.
Application of optical probes as an alternative technique for measurements in multiphase flow has the advantage of low cost, simplicity of setup and easy interpretation of results. The performance of optical probes has previously been investigated and was used to determine local void fraction (Cartellier, 1989; Juliá et al., 2005). Further application for measuring the bubble velocity and size has been carried out by Cartellier (1992). Two-point optical probes were also used in air water two-phase flows (Barrau et al., 1999).
Four-point optical fibre probes have been utilized to measure the gas fraction and velocity distribution as well as radial distributions of the bubble size (Frijlink, 1987; Mudde and Saito, 2001; Guet et al., 2003). Moreover, four-point optical fibre probes were used to determine bubble shape and orientation of ellipsoidal bubbles (Luther et al., 2004; Guet et al., 2005).
The objective of the present study is to investigate the performance of four-point optical fibre probes on the bubble velocity measurement in a bubble column. Furthermore, the influence of material properties of the liquid phase on the accuracy of the velocity determination is considered.

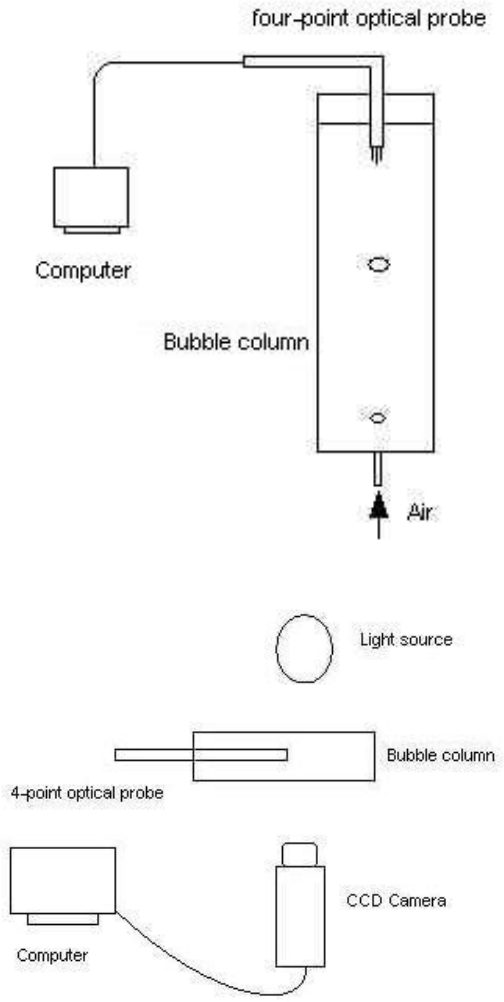

Figure 1: Sketch of experimental setup.

For this purpose, a simple experiment was designed. A high speed camera was used to record images of the approach of a bubble rising in a flat bubble column towards a four-point optical fibre probe and the subsequent piercing of the bubble by the tips of the probe. Meanwhile, signals generated by the four-point optical fibre probe were recorded simultaneously. Images taken by the camera and signals generated by the four-point optical fibre probe were processed afterwards separately. Velocities from the image processing were treated as reference velocities to evaluate the velocities obtained from the four-point optical fibre probe.
Five liquids with different material properties, including, viscosity, surface tension, density were used during measurements.

MEASUREMENT SYSTEM

Experimental setup

The experimental setup mainly consists of a small flat bubble column (10 x 110 x 500mm), an Imager Pro HS CMOS camera with 12 bit, 1024 x 1280 pixel resolution, a four-point optical probe, light source and computers, which is schematically shown in Figure 1.

The geometrical configuration of the probe tips is shown in Figure 2.

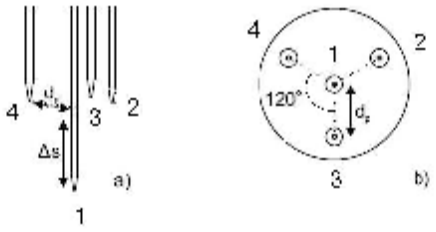

Figure 2: Geometry of four-point optical probe.

Table 1: List of physical properties of liquids.

	Density [kg/m^3]	Viscosity [mPa·s]	Surface tension [mN/m]
Water	998	1.00	72.75
Decane	730	0.838	23.37
Glycerol (60)	1153	10.7	66.9
Glycerol (72)	1187	27.6	66.5
Diethylene glycol	1120	30.2	44.77

The four-point optical probe is positioned at the top of the bubble column, a few centimetres below the liquid surface. The signals of the four-point optical probe are read with a LabView program and stored onto the hard disk simultaneously.
A high speed camera is mounted in front of the bubble column and a light source is illuminating the bubble column from behind, thus employing a shadowgraphy technique. Shadow images of the bubble and the four-point optical probe were recorded by the camera and stored on the computer. The image acquisition program is DaVis software from LaVision. The applied field of view of camera is 700x1024 pixels.
Five different liquids were used during measurements. The physical properties of each of the applied liquids were listed in Table 1.
An air bubble was released through a small hole with about 1 mm of diameter in the middle at the bottom of a flat bubble column. The range of produced bubble sizes is about 3 ~ 5 mm.

DATA PROCESSING

Image processing

The intensity images taken by the camera were processed with MatLab. In the image, a small region containing the bubble was cropped and then, an image segmentation method was employed within this small region to distinguish the bubble contours.
Image segmentation was based on the method of Otsu (1979), which is a nonparametric and unsupervised method of automatic threshold selection for picture segmentation. An optimal threshold was selected by the discriminant criterion, namely, maximizing the separability of the resultant classes in gray levels. A brief description of the method is as follows:
An image consists of L gray levels [1, 2, …, L] and the number of pixels at gray level i are denoted by n_i. Finally, the total number of pixels N is obtained by

summing n_i over all levels, $N = n_1 + n_2 + \ldots + n_L$. The fraction of pixels at level i is given by:

$$p_i = n_i / N\ ,\ \ p_i \geq 0 \tag{1}$$

$$\sum_{i=1}^{L} p_i = 1 \tag{2}$$

Suppose the pixels are dichotomized into two classes C_0 and C_1 (background and objects, or vice versa) by a threshold at level k. C_0 denotes pixels with levels [1, …, k], and C_1 denotes pixels with levels [k+1, …, L]. The probabilities of class occurrence, ω and the class mean levels, μ, respectively are given by

$$w_0 = \Pr(C_0) = \sum_{i=1}^{k} p_i = w(k) \tag{3}$$

$$w_1 = \Pr(C_1) = \sum_{i=k+1}^{L} p_i = 1 - w(k) \tag{4}$$

and

$$\begin{aligned} m_0 &= \sum_{i=1}^{k} i \Pr(i \mid C_0) = \sum_{i=1}^{k} i p_i / w_0 \\ &= m(k) / w(k) \end{aligned} \tag{5}$$

$$\begin{aligned} m_1 &= \sum_{i=k+1}^{L} i \Pr(i \mid C_1) = \sum_{i=k+1}^{L} i p_i / w_1 \\ &= \frac{m_T - m(k)}{1 - w(k)} \end{aligned} \tag{6}$$

The total mean level of original picture is:

$$m_T = m(L) = \sum_{i=1}^{L} i p_i \tag{7}$$

The between-class variance is given by:

$$\begin{aligned} s_B^2 &= w_0 (m_0 - m_T)^2 + w_1 (m_1 - m_T)^2 \\ &= w_0 w_1 (m_1 - m_0)^2 \end{aligned} \tag{8}$$

The threshold k^* that maximizes s_B^2 is treated as optimal threshold to segment the objects from the background in the image.

Sezgin and Sankur (2004) compared some image thresholding techniques and evaluated their performance quantitatively. By using several thresholding performance criteria, Otsu's method performed excellent for image segmentation within 40 image thresholding methods. Sezgin and Sankur also mentioned that Otsu's method can give satisfactory results when the numbers of pixels in each class are close to each other.

Properties of the bubble, such as area, centre of mass, perimeter, equivalent diameter, orientation, major axis length, minor axis length and so on, can be calculated through manipulating the pixels representing bubble in image. After this step, the coordinates of the centre of mass obtained from the cropped region were transformed back to the coordinates system of original image.

Subsequently, the vertical component of the bubble velocity can be calculated with the following equation in a sequence of image.

$$v_i = \frac{y_{i+1} - y_i}{\Delta t} \tag{9}$$

where y is the vertical coordinate of the centre of mass of the bubble and Δt is the time difference between two sequential images.

Two characteristic velocities were calculated separately. One is the average velocity before the bubble hits the probe, which will be termed the terminal velocity. The other characteristic velocity is the average velocity during the bubble-probe contact, which will be termed the piercing velocity. These two velocities will be used to compare with the velocity obtained from the four-point optical probe.

Signal processing of optical probe

The main task of the signal processing of the optical probe data is to identify the parts representing the bubble in the raw signal. That is, the moments of probe entry and exit through each bubble need to be found in each pulse. The idea to find the relevant moments is based on different levels in the raw data signal, i.e. the liquid level, the gas level and the noise level (Cartellier, 1992; Barrau et al., 1999; Harteveld, 2005). Pre-signals were observed in some bubble piercing events. In viscous liquids, such as glycerol solutions, the reason for these pre-signals is that the bubble surface is perpendicular as it approaches the tip. This leads to detectable reflections by the surface prior to piercing. In low viscosity liquids, wobbling behavior of bubbles with a moderate size may also result in the occurrence of a pre-signal. Therefore, a criterion based on the noise level to determine the entry time is debatable. Harteveld (2005) suggested that the threshold was set to 10% of the bubble plateau level. However, it is hard to remove pre-signals in this way if the signal-to-noise ratio of the probe is low.

In the present study, the entry and exit moments were determined with the following equations:

$$V_{entry} = V_L + 0.1(V_G - V_L) \tag{10}$$

$$V_{exit} = V_L - 0.1(V_G - V_L) \tag{11}$$

which was the same as the threshold used by Harteveld (2005). In some cases where a pre-signal occurs, additional processing was adopted. The entry point was selected manually at the very beginning of the ascending ramp after primary peak.

Based on above steps, the moments of probe entry and exit can be determined for each bubble. With such information, the time difference between upper surface of bubble hitting the longest tip and the other three tips can be derived.

The velocity of bubble was calculated by the following equation:

$$u = \frac{\Delta s}{\Delta t} = \frac{\Delta s}{\frac{1}{3}\sum \Delta t_i}, i = 1, 2, 3 \tag{12}$$

where Δs is the vertical distance between the longest tip and the other three tips. Δt_i is the time difference between hitting of the longest tip and short tip i.

Due to varying behaviour of the bubble during the interaction with the probe, these three time differences

may vary from one another. This is amongst others due to the bubble hitting the probe off-centre and irregular deformation of the upper bubble surface during the interaction. To reduce the error in the bubble velocity determination, the following selection criterion was used:

$$\left|\frac{\Delta t_i - \Delta t}{\Delta t}\right| < b, i = 1,2,3 \qquad (13)$$

Mudde and Saito (2001) and Fortunati et al. (2002) studied the influence of b on the accuracy of the bubble velocity numerically and experimentally. In Mudde's simulations, in case $8\% < \beta < 20\%$ the influence on the accuracy is negligible in comparison to other error sources. In Fortunati's experiment, no significant difference was observed on the average rise velocity and its standard deviation for $\beta < 25\%$. In the present single bubble experiments, $\beta = 30\%$ was adopted in order to allow more bubbles to be considered.

Uncertainty

In image processing, the uncertainty of instantaneous bubble velocity is related to the image acquisition rate, the determination of the centre of mass of the bubble and the applied magnification factor. The magnification factor was obtained by taking the diameter of the probe support as a reference length. The DaVis software was used to acquire images and the time interval between sequential images was very accurate. The accuracy of the centre of mass of the bubble depends on the performance of the image segmentation method. Assuming a maximum error of the image acquisition time of 10^{-6} s and a maximum error in the centre of mass of 0.5 pixel, the instantaneous bubble velocity has an uncertainty ranging of 6-7% before the probe piercing the bubble in each of the applied liquids. The uncertainty increases up to 13.5% in viscous liquids when the optical probe pierces the bubble. On the contrary, the uncertainty did not change much in low viscosity liquids when the optical probe pierces the bubble.

The uncertainty of the average bubble velocities was much smaller than that of the instantaneous velocity. The uncertainty in the terminal velocity ranged from 0.07% to 12.5%, whereas the uncertainty in the piercing velocity ranged from 1.2% to 22.5%.

The uncertainty in bubble diameter is mainly influenced by the method of image processing. The two major sources of error were related to the calculation of the area of the bubble and the magnification factor. Assuming a maximum error of 0.3% in the bubble area determination, the uncertainty in the bubble diameter varied from 0.3% to 9.5%.

Due to inaccuracies in the manufacturing of the probe, the length of the three short tips of the probe may not be exactly the same as designed. The distances between the longest tip and the other three short tips vary slightly. Furthermore, the three time differences used to calculate the velocity of bubble also varied because of unpredictable interaction between bubble and four-point optical probe. These two influences were considered to analyse the uncertainty of the bubble velocity obtained from the four-point optical probe, which ranges from 19% to 35%.

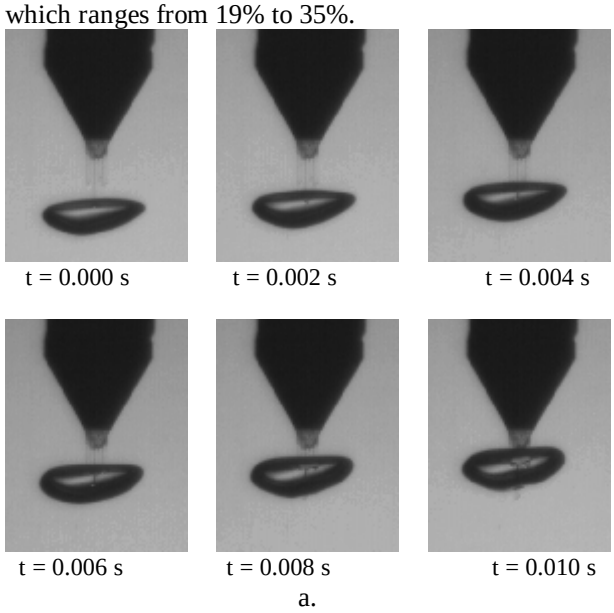

a.

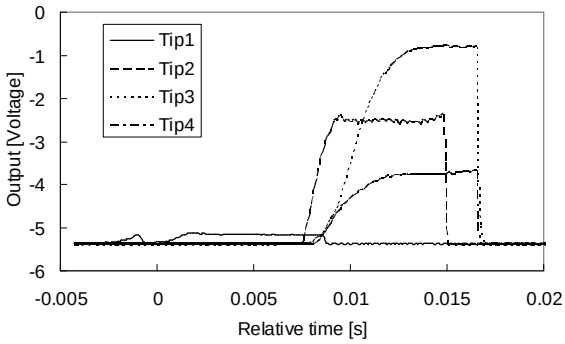

b.

Figure 3: Interaction between bubble and four-point optical fibre probe in air-decane system: **a**. images, **b**. corresponding signals.

RESULTS & DISCUSSION

Bubble deformation & signals of optical probe

Two different interactions between bubble and four-point optical probe are presented in figures 3 and 4.

Figure 3a shows the images recorded for the air-decane system. The wobbling bubble with relative high Reynolds number did not considerably change in shape during the interaction with the probe.

In figure 3.b, the signals generated by the four-point optical fibre probe are plotted. It can clearly be seen that a pre-signal exists in the signal of the longest tip. This may result from the movement of the bubble roof of the bubble. Irregular movement of the bubble roof may reflect the light back onto the fibre while it is still approaching the first tip.

In figure 4a, recordings of the piercing process of a bubble rising in an air-glycerol solution system are shown. Because of high viscosity of the glycerol solution, the bubble has an ellipsoidal shape. The piercing time is much longer than that in the air-decane system. The deformation of the bubble is clearly discernible. Since the four-point optical fibre probe was almost piercing the centre of the bubble, the flat roof

reflected some light back through the optical fibre. Thus, also in this case, a pre-signal for the longest tip is obtained.

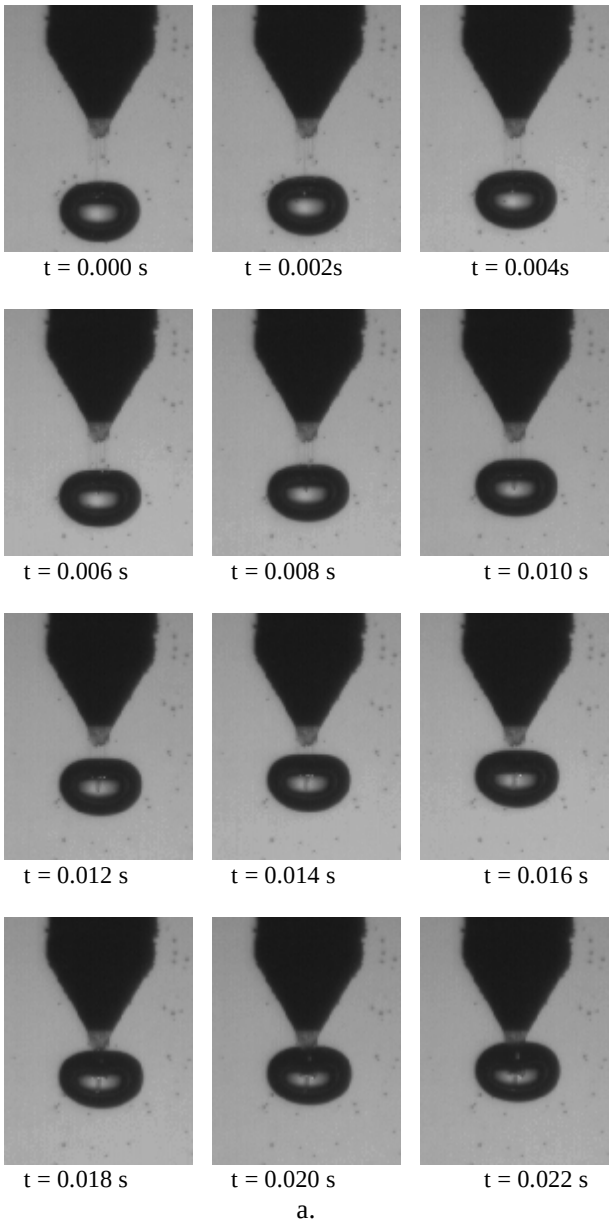

a.

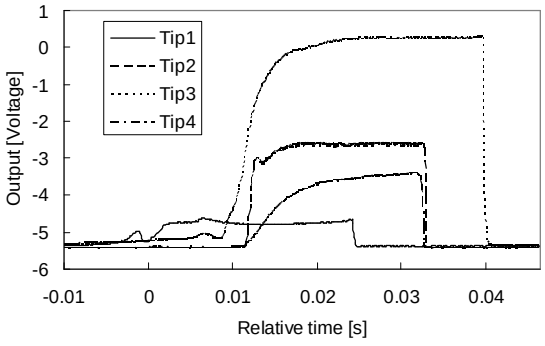

b.

Figure 4: Interaction between bubble and four-point optical fibre probe in air-glycerol solution (72%) system: **a**. images, **b**. corresponding signals.

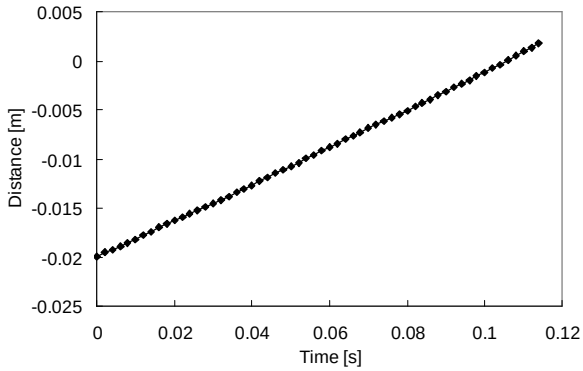

a.

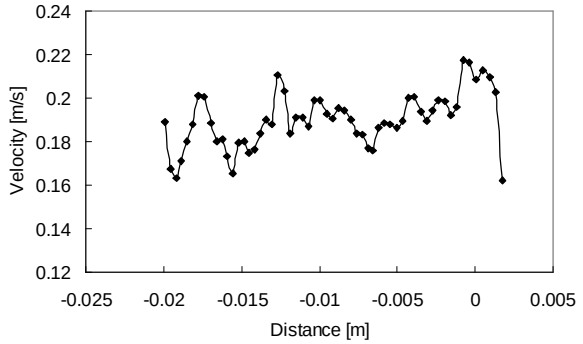

b.

Figure 5: Results from air-decane system: **a**. positions of rising bubble versus time, **b**. vertical velocity of rising bubble versus position.

Bubble rise velocity

Figures 5 and 6 show the instantaneous positions and velocities that were recorded with the CMOS camera. Note that in the plots, the origin of coordinates was put at the bottom of the longest tip of the four-point optical probe. In the top of both figures, it can be found that the vertical component of the bubble position increases approximately linearly with increasing time. Due to the effect of physical properties, such as viscosity, surface tension and the size of the bubble, the trajectories of the bubble in the low viscosity liquid are different from those of the bubble in the viscous liquid. In the low viscosity liquids, the bubble positions show more fluctuations compared to bubbles rising in viscous liquids because of wobbling behaviour, which is reflected in the corresponding velocity plots. Moreover, it is observed that in the low viscosity system the position and velocity trends start to deviate as soon as the bubble hits the tip. On the contrary, in the viscous liquid, the ellipsoidal shape of the bubble is affected during the interaction with the probe. As a result, the horizontal bubble diameter starts to increase slowly. Furthermore, it is clear that the presence of the probe has a retarding effect on the bubble rise velocity in a still liquid.

Nevertheless, the instantaneous velocities prior to piercing can be used to calculate the average terminal bubble velocity in liquids of both low and high viscosity.

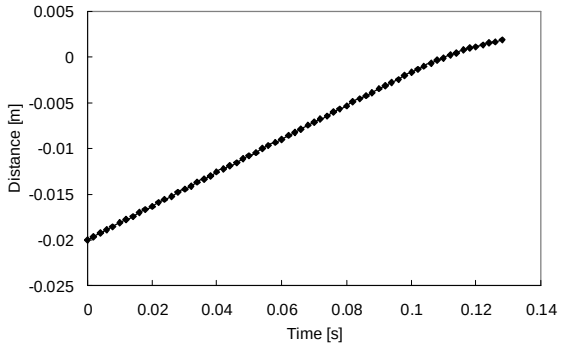

a.

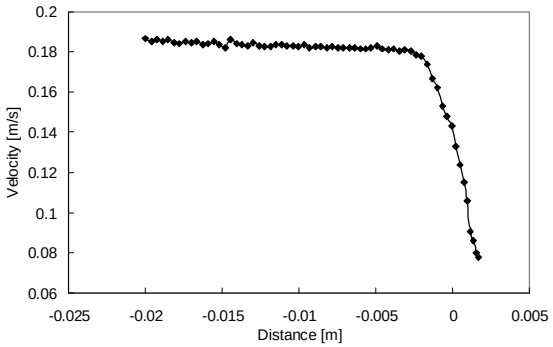

b.

Figure 6: Results from air-glycerol solution (72%) system: **a**. positions of rising bubble versus time, **b**. vertical velocity of rising bubble versus position.

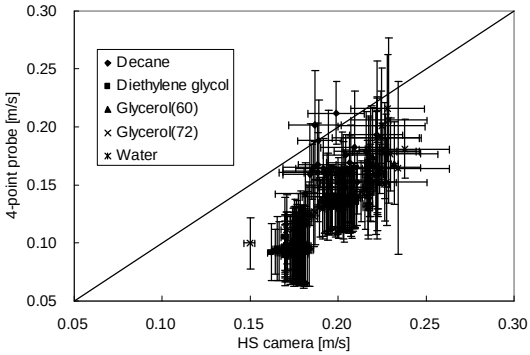

Figure 7: Parity plot of velocities from five air-liquid systems.

Comparisons of results

Figure 7 shows a parity plot of the results from both the image processing and signal processing of four-point optical probe. The straight line in the plot is identity. From the plot, it can be concluded that the presence of the four-point optical probe has a considerable effect on the probe velocity measurement in viscous liquids. In a viscous liquid the rising bubble behaves more or less stable until it hits the tips of four-point optical probe. The roof of bubble starts to deform while hitting tips of the probe, which clearly can be seen in the images. In the meantime, the large viscosity of the liquid also causes deceleration of the movement of bubble along the tip.

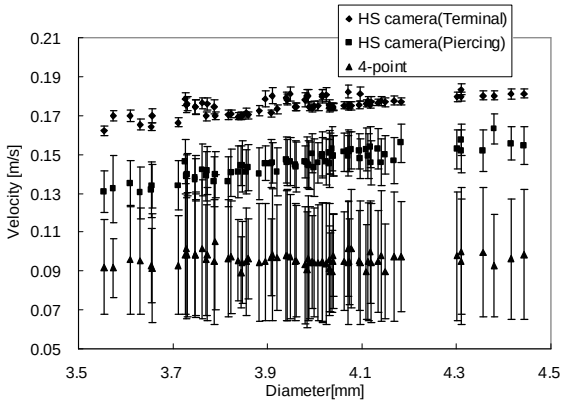

Figure 8: Comparisons of terminal velocity, piercing velocity and velocity from four-point optical fibre probe in air-diethylene glycol system.

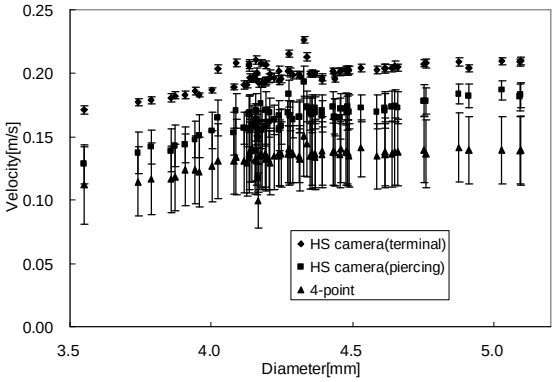

Figure 9: Comparisons of terminal velocity, piercing velocity and velocity from four-point optical fibre probe in air-glycerol solution (72%) system.

For low viscosity liquids, the velocities measured by the four-point optical probe are much closer to those obtained with the camera. A reasonable explanation for this would be that the bubble has already been in a wobbling state in the observation area. The shape of the bubble is already changing continuously when it hits the tips. The obstructing effect of the probe does not influence the bubble velocity significantly. However, because of the wobbling behaviour, the bubble velocity measured by the probe may be either smaller or larger than that from image processing, which makes determination of the bubble velocity with the probe more difficult.

Figures 8 to 10 show results for three velocities obtained from both the camera and the probe in different liquids. From the plots, it can be seen that the velocity deviation obtained from the probe is always the largest one. Whereas, velocities obtained by the camera in viscous liquid have the smallest deviations. This is because bubbles do not show large fluctuations when rising in a viscous liquid. The velocities obtained by the camera during piercing have moderate deviations in the three velocities. In those cases, the bubbles were decelerated and started to deform during the bubble-probe interaction. Furthermore, the extent of deceleration and deformation varies.

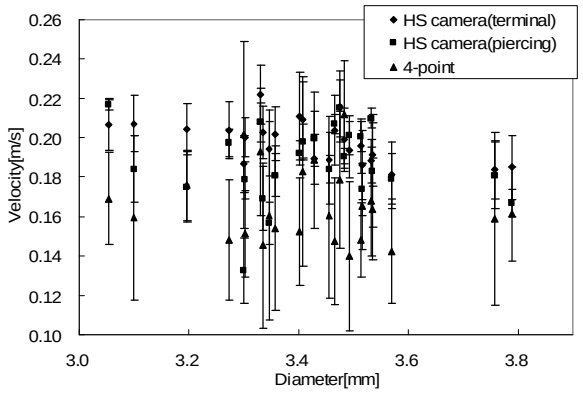

Figure 10: Comparisons of terminal velocity, piercing velocity and velocity from four-point optical fibre probe in air-decane system.

Table 2: Morton numbers and deviations in five liquids.

	Morton number	deviation (%)
Water	2.57×10^{-11}	19.5
Decane	5.18×10^{-10}	17.6
Glyerol (60%)	3.69×10^{-7}	28.7
Glyerol (72%)	1.64×10^{-5}	32.5
Diethylene glycol	8.11×10^{-5}	45.4

In diethylene glycol, the deviation between the terminal velocity and the velocity from the probe is ranging from 39% to 50%. In the glycerol solution (72 m% glycerol), the deviation is ranging from 27% to 36%. In the glycerol solution with 60 m% glycerol, the deviation is between 20% and 40%. The deviation in decane ranged from 0.3% to 28%. Finally, the deviation in water ranged from to 5% to 33%.

Analysis of the probe-camera deviation

The Morton number and average deviations between the terminal velocity and the velocity from the four-point optical fibre probe in five different liquids are listed in Table 2.

Figure 11 also shows the relationship of average deviation and Morton number in the five investigated liquids. Velocities measured in diethylene glycol by the probe have the highest deviation with those taken by CMOS camera within these five liquids. Whereas, the deviation measured in decane is the lowest one.

The order of magnitude of Reynolds number is about 10^3 in water and about 10^2 in decane. In these cases, the influence of viscous forces is much smaller than the inertial force acting on the bubble. Therefore, viscous forces do not dominate in the range of the investigated Reynolds numbers. As a result the probe has little influence on the motion of the bubble. The deviation in water is slightly larger than that in decane. This could be because the surface tension of water is larger than that of decane. A large surface tension will hamper the piercing of the bubble.

In measurements in viscous liquids, the order of magnitude of the Reynolds number is about 10. In this case, viscous forces have a significant influence on the motion of the bubble. Therefore, the deviations between terminal velocity and velocity from four-point optical probe were larger.

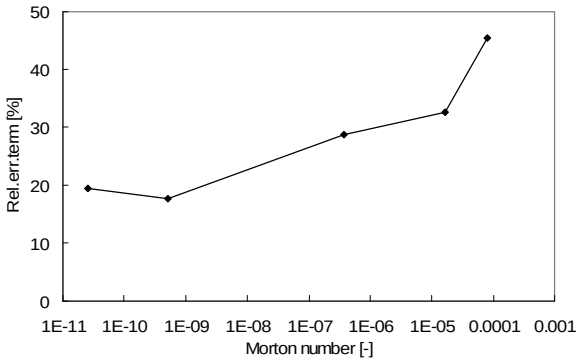

Figure 11: Plot of deviation between terminal velocity and velocity from four-point optical fibre probe versus Morton number.

CONCLUSIONS

The presented work was dedicated to investigate the performance of a four-point optical probe on the determination of the bubble velocity in a bubble column and the influence of material properties on the accuracy of a four-point optical probe. For this purpose, a combined experiment was designed. A CMOS camera was used to verify the performance of the four-point optical probe. Five liquids with different physical properties were employed. The following conclusions are drawn from this work.

First of all, the motion of the bubbles was more or less stable when rising in bubble column for the investigated systems. Therefore, the instantaneous velocities from image processing have been averaged for further comparison with the velocity measured by the optical probe.

Second of all, the presence of the probe can influence motion of bubble in bubble column, which results in discrepancy of prediction of velocity with four-point optical probe.

Third of all, physical properties of liquid, such as, viscosity and surface tension, can influence performance of four-point optical probe. The Reynolds number and Morton number can be combined to describe the extent of discrepancy between terminal velocity and prediction from four-point optical probe. In the viscous dominant regime (low Reynolds), the deviation is large when the Morton number increases. When viscosity does not dominate the motion of the bubble (high Reynolds), the Morton number is low and the surface tension will influence the accuracy in the velocity measurement of the probe.

In short, by applying four-point optical fibre probe in bubble column, inaccuracies with respect to bubble velocities cannot be avoided. Particularly, the discrepancy becomes large when the viscosity of liquid increases. However, based on the fact of the stable behavior of bubble rising in viscous liquid, correction for velocity obtained from four-point optical fibre probe may be possible. Furthermore, in low viscosity liquid systems (i.e. high Reynolds), this inaccuracy is lowest. For high void fraction bubbly flow in a bubble column

at low liquid velocities, where PIV or LDA may not work ideally, the four-point optical probe would also be an appropriate option.

REFERENCES

Barrau, E. et al., (1999), "Single and double optical probes in air-water two-phase flows: real time signal processing and sensor performance", *International journal of Multiphase Flow*, **25**, 229-256.

Bröder, D. and Sommerfeld, M., (2002), "An advanced LIF-PLV system for analysing the hydrodynamics in a laboratory bubble column at higher void fractions", *Experiments in Fluids*, **33**, 826-837.

Cartellier, A., (1989), "Optical probes for local void fraction measurements: Characterization of performance", *Rev. Sci. Instrum.*, **61(2)**, 874- 886.

Cartellier, A., (1992), "Simultaneous void fraction measurement, bubble velocity, and size estimating using a single optical probe in gas-liquid two-phase flows", *Rev. Sci. Instrum*, **63(11)**, 5442-5453.

Deen, N.G. (2001), "An experimental and computational study of fluid dynamics in gas-liquid chemical reactors", PhD thesis, Aalborg University, Denmark.

Juliá, J.E. et al. (2005), "On the accuracy of the void fraction measurements using optical probes in bubbly flows", *Rev. Sci. Instrum.*, **76**, 035103, 1-13.

Fortunati, R.V. et al. (2002), "Accuracy and feasibility of bubble dynamic measurements with four-point optical fiber probes", 11th International symposium, Lisbon, Portugal, July 8-11.

Frijlink, J.J., (1987), "Physical aspects of gassed suspension reactors", PhD thesis, Delft University of Technology, The Netherlands.

Guet, S. et al., (2003), "Bubble velocity and size measurement with a four-point optical fiber probe", *Part. Part. Syst. Charact.*, **20**, 219-230.

Guet, S. et al., (2005), "Bubble shape and orientation dtermination with a four-point optical fibre probe", *Experimental Thermal and Fluid Science*, **29**, 803-812.

Harteveld, W., (2005), "Bubble columns: Structure or Stability?", PhD thesis, Delft University of Technology, The Netherlands.

Lindken, R. and Merzkirch, W., (1999), "Velocity measurements in multiphase flow by means of particle image velocimetry", *Chem. Eng. Technol.*, **22**, 202-206.

Luther, S. et al., (2004), "Bubble aspect ration and velocity measurement using a four-point fiber-optical probe", *Experiments in Fluids*, 36, 326-333.

Mudde, R. and Saito, T., (2001), "Hydrodynamical similarities between bubble column and bubbly pipe flow", *J. Fluid. Mech*, **437**, 203-228.

Otsu, N. (1979), "A threshold selection method from gray-level histograms", *IEEE Transactions on System, Man and Cybernetics*, **9(1)**, 62-65.

Sezgin, M. and Sankur, B., (2004), "Survey of image thresholding techniques and quantitative performance evaluation", *Journal of Electronic Imaging*, **13(1)**, 146-165.